Indian Journal of Ecology (2024) 51(1): 01-13
DOI: https://doi.org/10.55362/IJE/2024/4189

Manuscript Number: 4189
NAAS Rating: 5.38

Spatio-temporal Reconstruction of MODIS Land Surface Temperature over Samastipur district, Bihar with GLDAS using Geo-Matics

G.M. Rajesh, Sudarshan Prasad[1] and I.B. Bhagat[1]

Department of Soil and Water Conservation Engineering, KCAET, Kerala Agricultural University, Thrissur-680 656, India
[1]Department of Soil & Water Engineering, CAE, RPCAU, Pusa, Samastipur-848 125, India
E-mail: rajeshgm7991@gmail.com

Abstract: Present study aims to estimate LST using GLDAS monthly satellite product over Samastipur district of Bihar using Geomatics. The monthly dataset of LST products of 0.25° × 0.25° grid size for the period of 21 years from 2000 to 2020 were downloaded and monthly LST values were extracted, compared and validated with ground-based Temperature measured at MS, Pusa. Bias in extracted climatic variables was identified and was corrected using linear scaling. The spatial and temporal distribution of LST were developed using inverse distance weighted interpolation (IDW) technique of ArcGIS. The estimated LST values are in good agreement with temperature observed at MS, Pusa with correlation coefficient of 95.56%. The estimated LST was highest in June (30.75°C) and lowest in January (14.39 °C) and gradually increased to July and followed by decreasing trend from July to December.

Keywords: LST, Bias correction, ArcGIS, Spatio-temporal distribution

Land surface temperature (LST) plays a crucial role in regulating regional and global surface energy exchange and the interaction between land and the atmosphere Monitoring LST and understanding its spatio-temporal changes at various scales are essential for comprehending the response of natural ecosystems to climate change and human activities (Li et al 2013, Zeng et al 2015, Li and Wang 2019). LST has found wide applications in climate change assessments, agricultural drought monitoring, urban heat analysis, and land surface modelling Moreover, the Global Climate Observing System (GCOS) recognizes LST as an essential climate variable (ECV) due to its significant influence on Earth's climate characterization. To acquire accurate LST data across different spatial scales, remote sensing techniques offer a valuable solution. They provide extensive spatial coverage, frequent data acquisition, long-term observations, and superior performance compared to ground-based measurements (Chung et al 2020). Among remote sensing methods, thermal infrared (TIR) measurements offer higher spatial resolution and accuracy than passive microwave (MW) sensors, making TIR-based estimations the preferred choice for LST monitoring. The availability of meteorological data has some drawbacks, such as incompleteness, a small area of coverage, and sporadic missing observations. These limitations make it very difficult to study climate science and its processes in depth. On the other hand, satellite-based data provides a valuable resource in the form of extensive and long-term images capturing these variables. However, extracting meaningful information from these satellite images remains a challenging task. Considering above challenges present study is under taken to estimate LST from satellite products using GIS environment.

MATERIAL AND METHODS

Study area: Samastipur district of Bihar is spread between 25° 30" to 26° 05" N latitudes and 85° 37' 50" to 86° 23' 30" E longitude over an area of 2904 km^2, lies about 52 m above mean sea level. The district is surrounded on the north by the Bagmati River, which divides it from Darbhanga, on the west with Vaishali and parts of Muzaffarpur districts, on the south by the Ganges, and on the east by Begusarai and a few parts of Khagaria districts. The primary rivers in the area are the Burhigandak and Ganga, which provide the majority of the drainage.

Climate: The district is located in the monsoon tropical zone and has a semi-arid to subtropical climate. The temperature ranges from 6 °C in winter to 45°C in summer. The annual rainfall varies from 1100 mm to 1250 mm. The soil has a light to clay texture and suitable for growing rice, maize, wheat, pulses, oilseeds, tobacco, sugarcane, spices and vegetables. Pre-monsoon ground water levels range from 7.2 to 11.10 m bgl, whereas post-monsoon levels range from 3.2 to 6.4 m bgl.

Soil type and cropping pattern: Samastipur is located in the state's Agro-ecological zone-I, which is the North-West

alluvial plains. Samastipur is well-known for its rich alluvial soil and Rabi crops. The soil is clay loam with a relatively high organic matter content, making it ideal for growing vegetables and spices. The pH of the soil ranges between 5.8 to 8.0. They have a light texture with free $CaCO_3$ levels ranging from 3 to 10%. Rice, wheat, and maize are the most important crops in this region, followed by sugarcane and potatoes.

GLDAS Noah land surface temperature data characteristics: Global Land Data Assimilation System (GLDAS) Noah land surface temperature data product (GLDAS-2.1) Noah0.25° monthly dataset was downloaded (https://daac.gsfc.nasa.gov/) from the years 2000 to 2020 (Wan Z 2006) and processed in ArcGIS for land surface temperature extraction over the study area.

Climatic variables observed at meteorological station: The climatic variables such as daily rainfall and temperature (maximum and minimum) and sunshine hour data were collected from the meteorological station (MS) of RPCAU, Pusa for the 21 years from 2000 to 2021. These daily data were processed and converted into monthly scale for validating the satellite based LST extracted from GLDAS (Phan and Kappas 2018).

Data Analysis

ArcGIS: The Environmental Systems Research Institute developed ArcGIS (V 10.7.1) software, a geographic information system (GIS) for working with maps and geographic data was used to, compile, analyse geographic data, and prepare thematic maps. The monthly land surface temperature of 21 years (2000 to 2020) were extracted from GLDAS 2.1 product with the help of a model developed in model builder tool of ArcGIS.

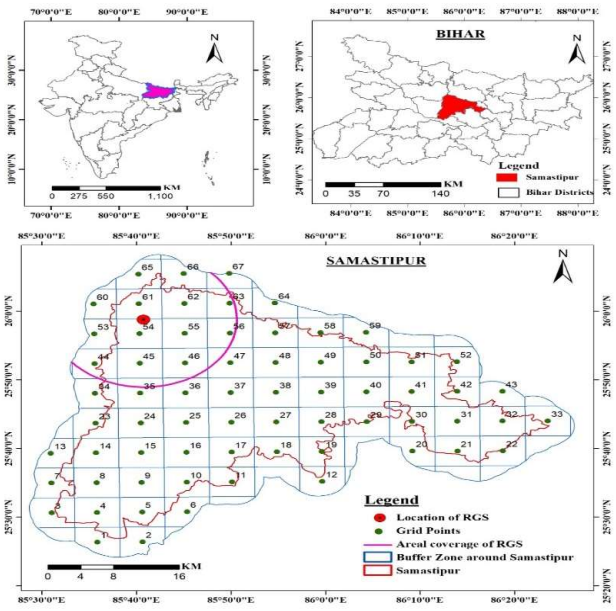

Fig. 1. Location of the study area

Extraction of climatic variables: Monthly GLDAS land surface temperature was extracted in ArcGIS for each grid point over the study area using a technique of which the flow chart is mentioned below (Fig. 2).

Comparison and validation using statistical approach: LST extracted from GLDAS LST 2.1 products were analysed and validated with the temperature measured at the meteorological station (MS), Pusa using statistical techniques. Various commonly used statistical measures such as Pearson correlation coefficient (PCC), mean error (ME), root mean square error (RMSE), bias (B), and percent bias (PB) were used to test the closeness between the climatic variables measured at MS, Pusa and satellite-based climatic variables. (Prasad et al 2012, Prasad and Kumar 2013, Ahmed et al 2015, Parinussa et al 2016, Bayissa et al 2017 and Singh et al 2017). Bias in extracted climatic variables was identified using statistical analysis and was corrected using linear scaling.

Spatio-temporal analysis: 21 years (2000 to 2020) monthly mean LST for all grid point over the study area were estimated and spatio temporal distribution maps were developed using inverse distance weighted interpolation technique of ArcGIS (Yang et al 2004 and Mayer et al 2016).

RESULTS AND DISCUSSION

The study region, Samastipur district of Bihar, was divided into 67 numbers of square grids of 8 km × 8 km spatial resolution using the Geographic Information System (ArcGIS) software version 10.7.1 (Fig. 2). The mean monthly land surface temperature over the study area was extracted from GLDAS LST products for each grid points created in the region using the algorithm and compared with ground base rainfall and air temperature recorded at meteorological station (MS), Pusa. Due to poor network of meteorological stations in the district, one available in the premises of Dr. Rajendra Prasad Central Agricultural University, Samastipur, Pusa was selected for comparison and validation. Following the suggestion of Subramanya, (2006) the observed and satellite-based rainfall and temperature over the selected grid points like GP-44, GP-45, GP 46, GP-47, GP-53, GP-54, GP-55, GP-56, GP-60, GP-61, GP-62, GP-63, GP-65 and GP-66 which are under the circumferential coverage of 3000 km^2 in flat area from MS, Pusa considering as center was considered for comparison and validation.

The basic statistics of air temperature recorded at MS, Pusa and land surface temperature extracted from GLDAS LST and bias corrected land surface temperature were determined (Table 1). The long term (from 2000 to 2020)

mean, standard deviation (SD) and coefficient of variation (CV) of observed air temperature were 24.95ºC, 5.63ºC and 0.226 over the grid points GP-44, followed by GP-45, GP 46, GP-47, GP-53, while the mean, SD, and CV of land surface temperature extracted from GLDAS LST were observed to be 25.94 ºC, 7.03 ºC and 0.271 over the grid points.

After applying the linear scaling to land surface temperature extracted from GLDAS LST using equation Eq. 3.5, the mean, SD, and CV of bias free land surface temperature was 24.95 ºC, 5.68 ºC and 0.228 over the grid points GP-44, GP-45, GP 46, GP-47, GP-53, GP-54, GP-55, GP-56, GP-60, GP-61, GP-62, GP-63, GP-65 and GP-66 (Table 1).

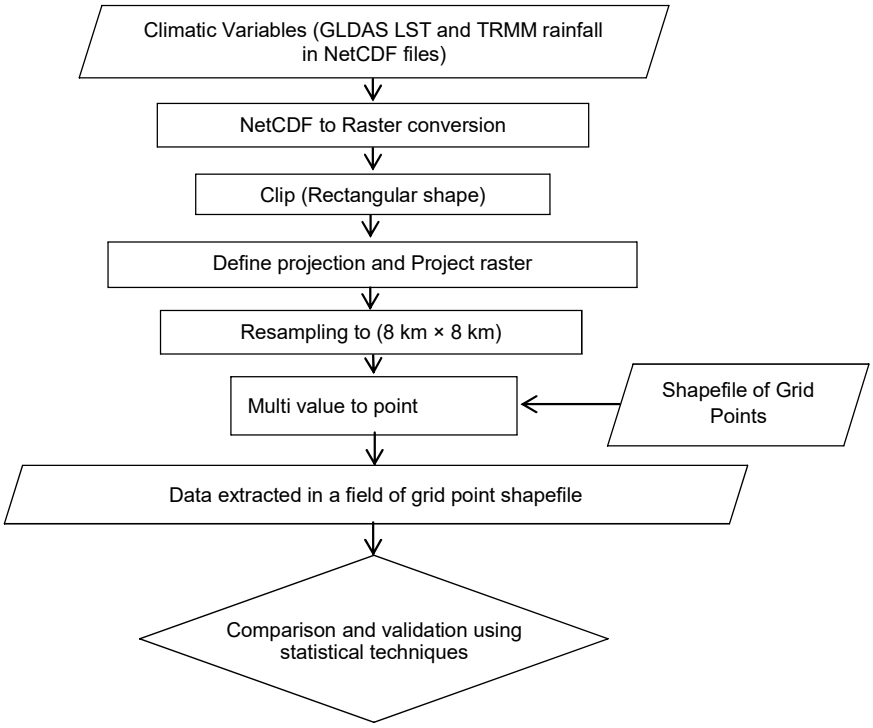

Fig. 2. Flow chart for extraction of climatic variables from satellite over the study area

Table 1. Basic statistics of observed air temperature, extracted and bias free GLDAS land surface temperature over Samastipur district of Bihar

Grid points	Observed air temperature			Extracted GLDAS LST			Bias corrected GLDAS LST		
	Mean (ºC)	SD (ºC)	CV	Mean (ºC)	SD (ºC)	CV	Mean (ºC)	SD (ºC)	CV
GP-44	24.95	5.63	0.23	25.94	7.03	0.27	24.95	5.68	0.23
GP-45	24.95	5.63	0.23	25.90	7.01	0.27	24.95	5.68	0.23
GP-46	24.95	5.63	0.23	25.86	6.97	0.27	24.95	5.68	0.23
GP-47	24.95	5.63	0.23	25.82	6.94	0.27	24.95	5.68	0.23
GP-53	24.95	5.63	0.23	25.83	7.00	0.27	24.95	5.68	0.23
GP-54	24.95	5.63	0.23	25.80	6.97	0.27	24.95	5.68	0.23
GP-55	24.95	5.63	0.23	25.76	6.94	0.27	24.95	5.68	0.23
GP-56	24.95	5.63	0.23	25.73	6.90	0.27	24.95	5.68	0.23
GP-60	24.95	5.63	0.23	25.67	7.00	0.27	24.95	5.68	0.23
GP-61	24.95	5.63	0.23	25.64	6.98	0.27	24.95	5.68	0.23
GP-62	24.95	5.63	0.23	25.61	6.94	0.27	24.95	5.68	0.23
GP-63	24.95	5.63	0.23	25.59	6.89	0.27	24.95	5.68	0.23
GP-65	24.95	5.63	0.23	25.48	6.98	0.27	24.95	5.68	0.23
GP-66	24.95	5.63	0.23	25.46	6.94	0.27	24.95	5.68	0.23

Graphical comparison: The monthly time series of mean air temperature observed at MS, Pusa, land surface temperature extracted from GLDAS LST, and bias free land surface temperature for grid points from GP-44 followed by GP-45, GP 46, GP-47 (Fig. 3). Similar patterns between observed air temperature and land surface temperature extracted from GLDAS LST were observed baring some extreme values in the figures of each grid points in the study area (Fig. 3). After applying linear scaling, extreme values of land surface temperature extracted from GLDAS LST were adjusted and overlying pattern between the near surface air temperature and the bias free land surface temperature extracted from GLDAS LST image were observed (Fig. 3). The land surface temperature extracted from the satellite for each grid points under the study area were compared with the respective air temperature measured at MS, Pusa. The root mean square error (RMSE), bias (B), Pearson correlation coefficient (PCC) and mean error (ME) between the land surface temperature extracted from the satellite and the air temperature measured at the meteorological station for each grid points under the study area were computed (Table 2).

The scatter plots between the near surface air temperature observed at MS, Pusa and the land surface temperature extracted from GLDAS LST over grid points from GP-44, GP-45, GP 46, GP-47, GP-53, GP-54, GP-55, GP-56, GP-60, GP-61, GP-62, GP-63, GP-65 and GP-66 (Fig. 4). These graphs clearly showed the over estimation of land surface temperature over the near surface air temperature observed at MS, Pusa. The extremely high values of land surface temperature extracted from GLDAS LST can easily be seen from the figures. The slope and the value of R^2 of fitted line of linear regression between the near surface air temperature observed at MS, Pusa and the land surface temperature extracted from GLDAS LST were in the range of 1.163 (GP-66) to 1.177 (GP-44) and 0.887 (GP-44 and GP-47) to 0.892 (GP-65), respectively (Table 2). The multiplying factors over the selected grid points were determined and the bias free monthly series of land surface temperature was obtained (Deo and Sahin 2017). The scatter plots between the near surface air temperature observed at MS, Pusa and the bias free land surface temperature over grid points from GP-44 to 47, 53 to 56,60 to 63, 65 and 66 (Fig. 5). These regression line fitted between the near surface air temperature observed at MS, Pusa and the bias free (corrected) land surface temperature lie over the line of best fit. The slope and the value of R^2 of linear regression between the mean air temperature observed and the bias free land surface temperature were greatly improved and was 0.987 and more than 0.955, respectively for all grid points over MS, Pusa (Table 2).

The average multiplying factors (AMF) of linear scaling for each month (January to December) were obtained by taking the average values of multiplying factors determined for each of the grid points mentioned above and were varied from 1.0086 (January) to 1.0141(December). Thus, the bias free

Table 2. Statistics of comparison between observed air temperature and land surface temperature over Samastipur district of Bihar

Grid points	Before Bias Correction of LST						After Bias Correction of LST					
	PCC	Bias	ME (ºC)	RMSE (ºC)	Linear Regression		PCC	Bias	ME (ºC)	RMSE (ºC)	Linear Regression	
					Slope	R^2					Slope	R^2
GP-44	0.940	1.040	0.990	2.740	1.177	0.887	0.980	1.000	0.000	1.200	0.987	0.955
GP-45	0.940	1.040	0.950	2.710	1.173	0.888	0.980	1.000	0.000	1.200	0.987	0.955
GP-46	0.940	1.040	0.910	2.680	1.167	0.888	0.980	1.000	0.000	1.200	0.987	0.956
GP-47	0.940	1.030	0.870	2.640	1.161	0.887	0.980	1.000	0.000	1.200	0.987	0.956
GP-53	0.940	1.040	0.880	2.670	1.172	0.889	0.980	1.000	0.000	1.190	0.987	0.956
GP-54	0.940	1.030	0.850	2.640	1.169	0.889	0.980	1.000	0.000	1.190	0.987	0.956
GP-55	0.940	1.030	0.810	2.610	1.162	0.889	0.980	1.000	0.000	1.190	0.987	0.956
GP-56	0.940	1.030	0.780	2.580	1.155	0.888	0.980	1.000	0.000	1.190	0.987	0.956
GP-60	0.940	1.030	0.720	2.610	1.174	0.890	0.980	1.000	0.000	1.190	0.987	0.956
GP-61	0.940	1.030	0.690	2.590	1.170	0.891	0.980	1.000	0.000	1.190	0.987	0.956
GP-62	0.940	1.030	0.660	2.560	1.162	0.890	0.980	1.000	0.000	1.180	0.987	0.957
GP-63	0.940	1.030	0.630	2.540	1.155	0.889	0.980	1.000	0.000	1.180	0.987	0.957
GP-65	0.940	1.020	0.530	2.540	1.172	0.892	0.980	1.000	0.000	1.180	0.987	0.957
GP-66	0.940	1.020	0.510	2.520	1.163	0.891	0.980	1.000	0.000	1.180	0.987	0.957

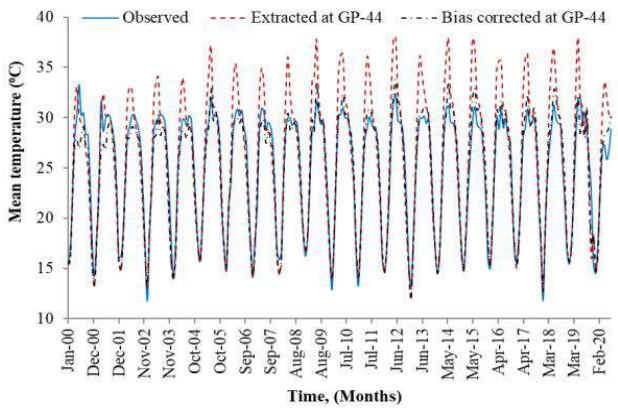
Observed
Extracted at GP-44
Bias corrected at GP-44
Mean temperature (°C)
Time, (Months)

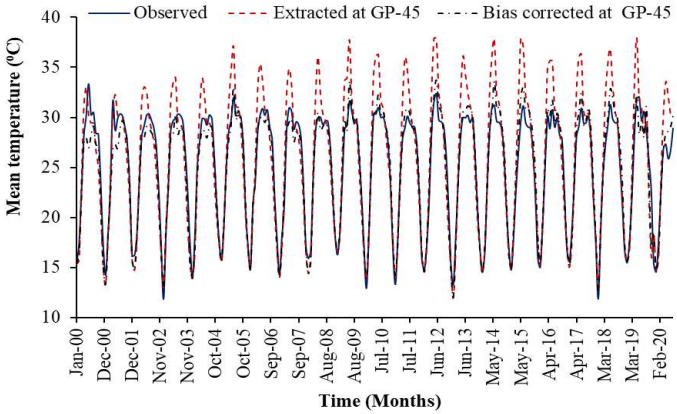
Observed
Extracted at GP-45
Bias corrected at GP-45
Mean temperature (°C)
Time (Months)

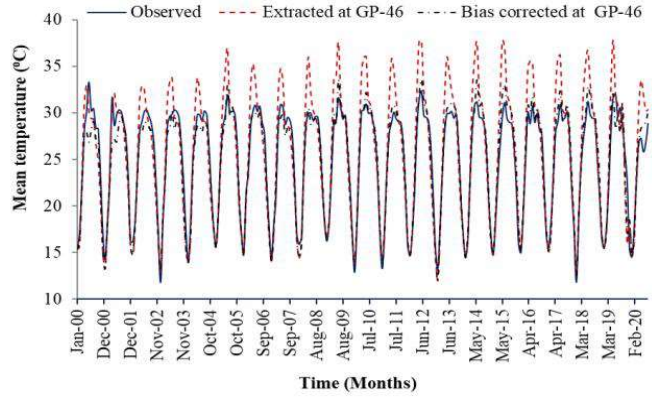
Observed
Extracted at GP-46
Bias corrected at GP-46
Mean temperature (°C)
Time (Months)

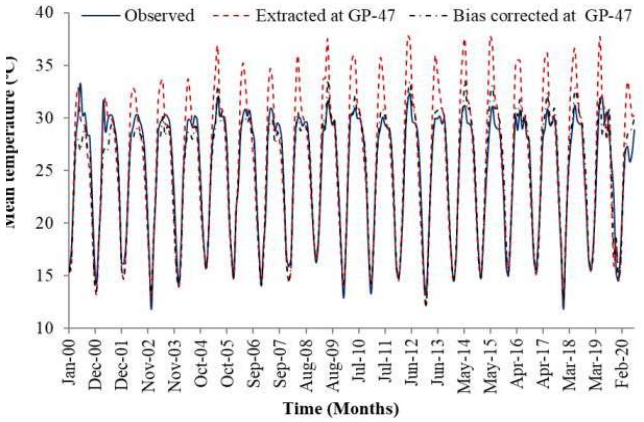
Observed
Extracted at GP-47
Bias corrected at GP-47
Time (Months)

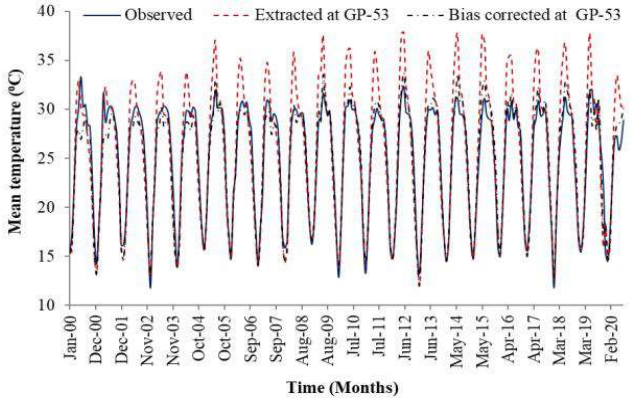
Observed
Extracted at GP-53
Bias corrected at GP-53
Mean temperature (°C)
Time (Months)

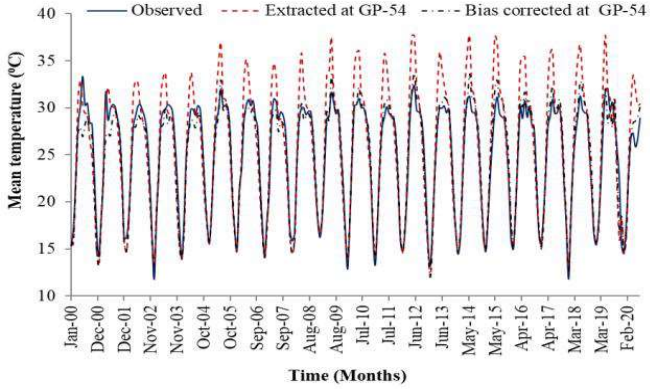
Observed
Extracted at GP-54
Bias corrected at GP-54
Mean temperature (°C)
Time (Months)

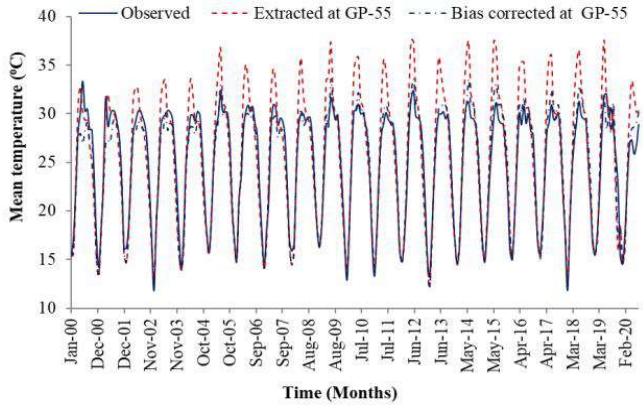
Observed
Extracted at GP-55
Bias corrected at GP-55
Mean temperature (°C)
Time (Months)

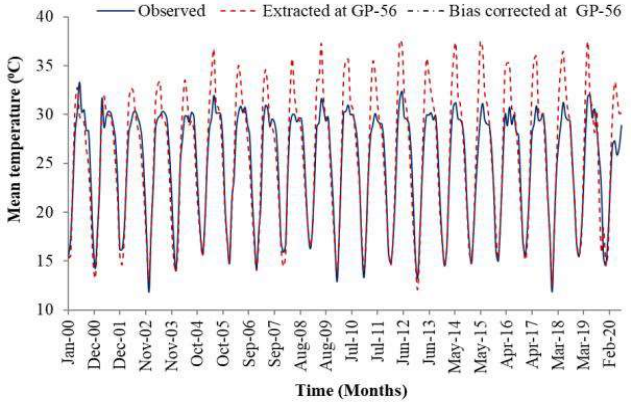
Observed
Extracted at GP-56
Bias corrected at GP-56
Mean temperature (°C)
Time (Months)

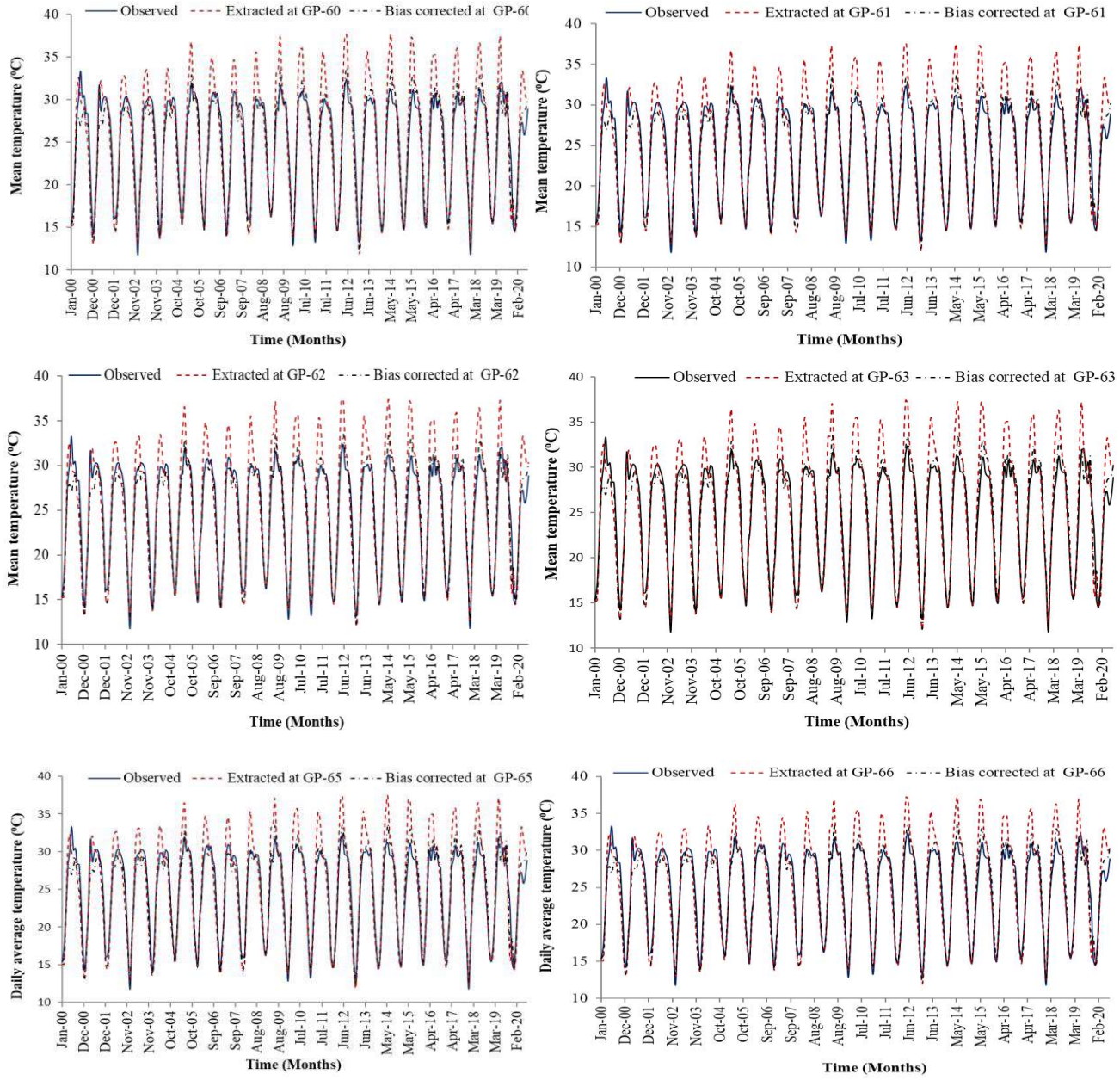

Fig. 3. Time series of mean temperature observed, extracted from LST image and bias corrected LST at grid points

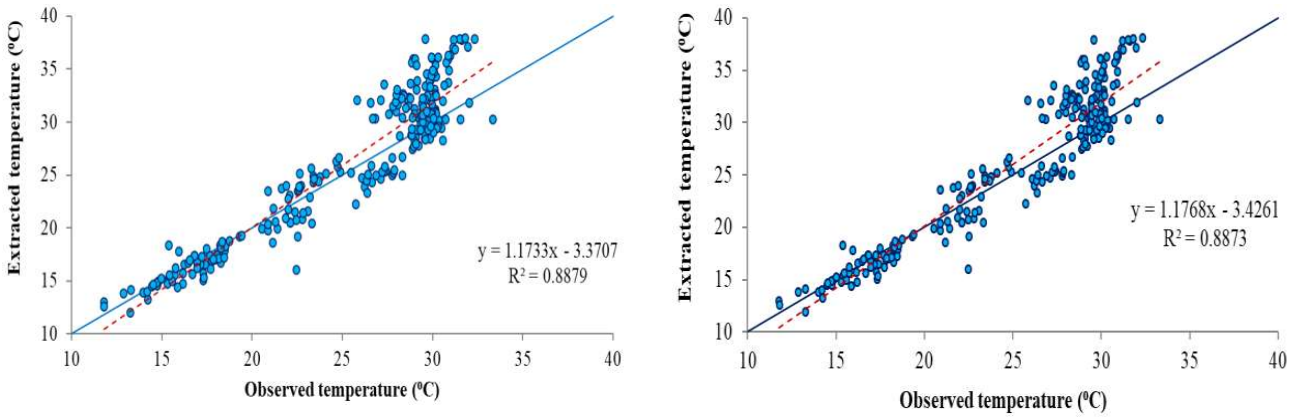

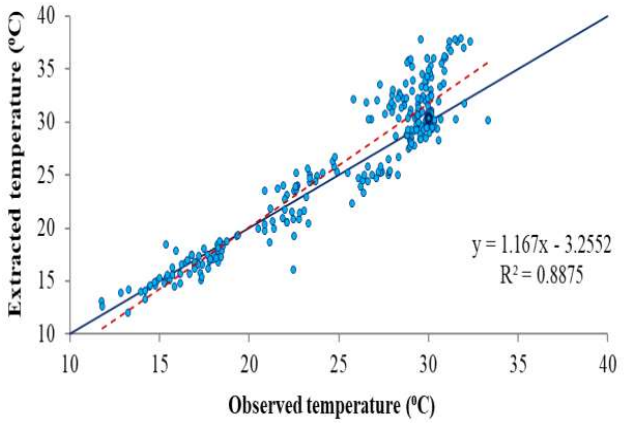
Extracted temperature (ºC)
Observed temperature (ºC)
y = 1.167x - 3.2552
R² = 0.8875

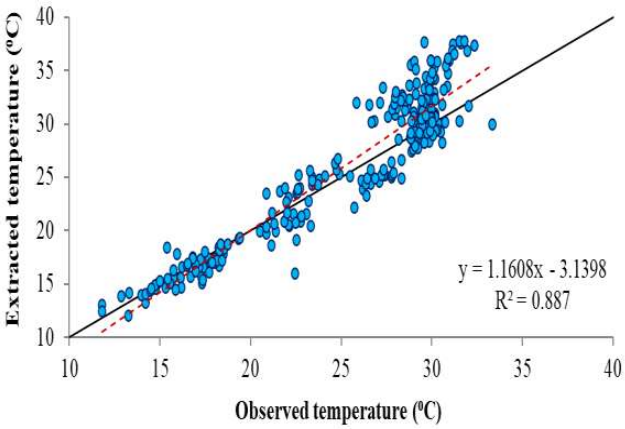
Extracted temperature (ºC)
Observed temperature (ºC)
y = 1.1608x - 3.1398
R² = 0.887

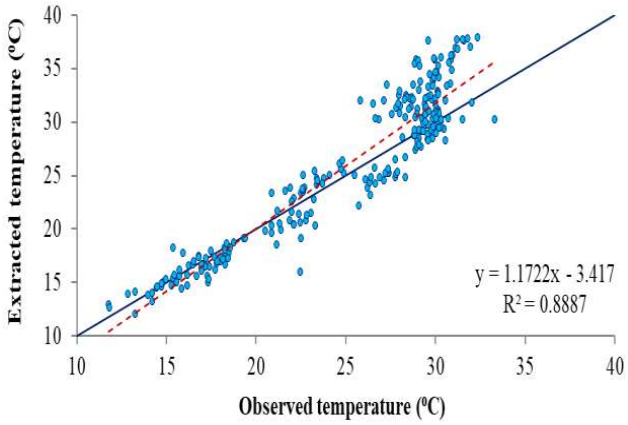
Extracted temperature (ºC)
Observed temperature (ºC)
y = 1.1722x - 3.417
R² = 0.8887

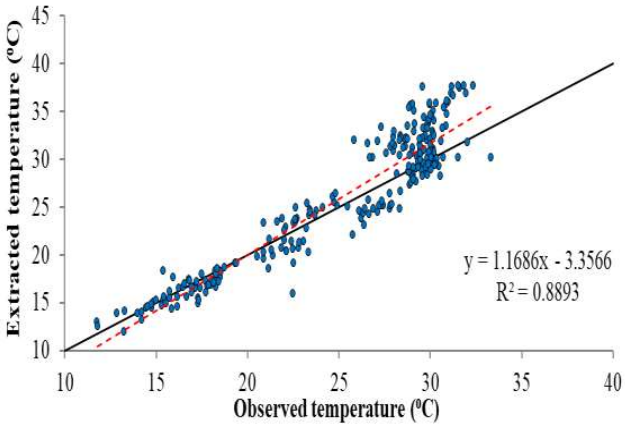
Extracted temperature (ºC)
Observed temperature (ºC)
y = 1.1686x - 3.3566
R² = 0.8893

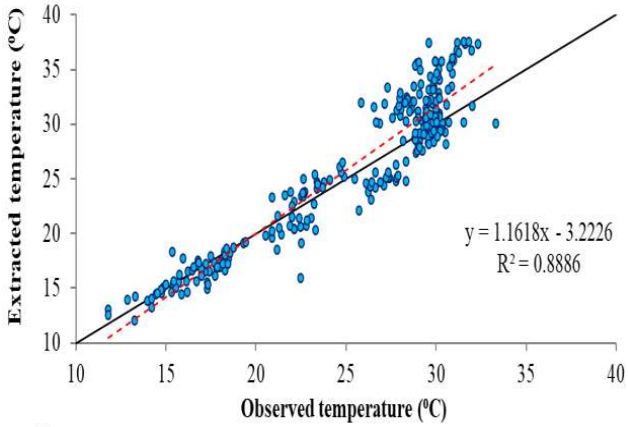
Extracted temperature (ºC)
Observed temperature (ºC)
y = 1.1618x - 3.2226
R² = 0.8886

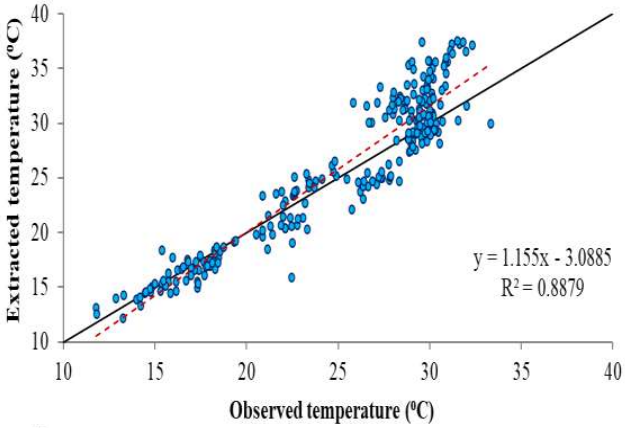
Extracted temperature (ºC)
Observed temperature (ºC)
y = 1.155x - 3.0885
R² = 0.8879

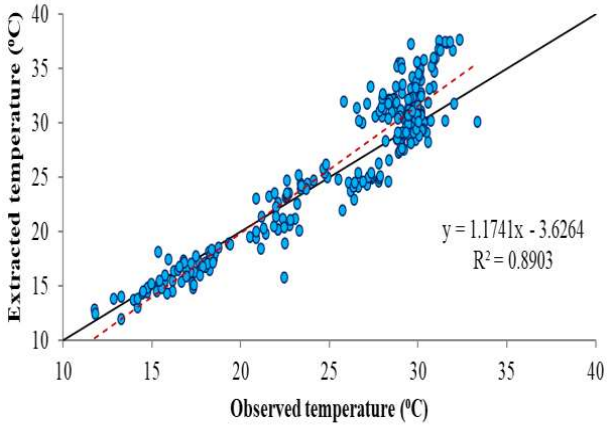
Extracted temperature (ºC)
Observed temperature (ºC)
y = 1.1741x - 3.6264
R² = 0.8903

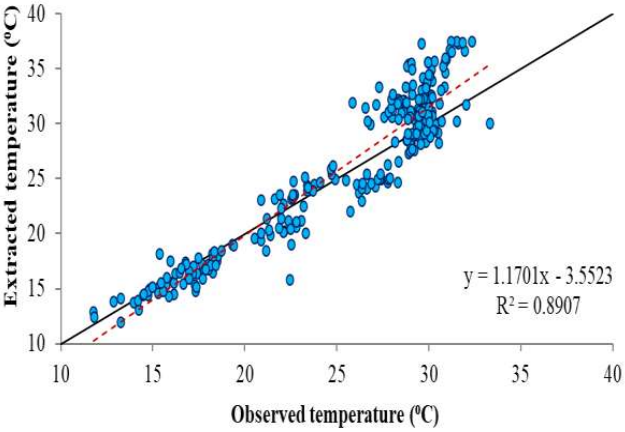
Extracted temperature (ºC)
Observed temperature (ºC)
y = 1.1701x - 3.5523
R² = 0.8907

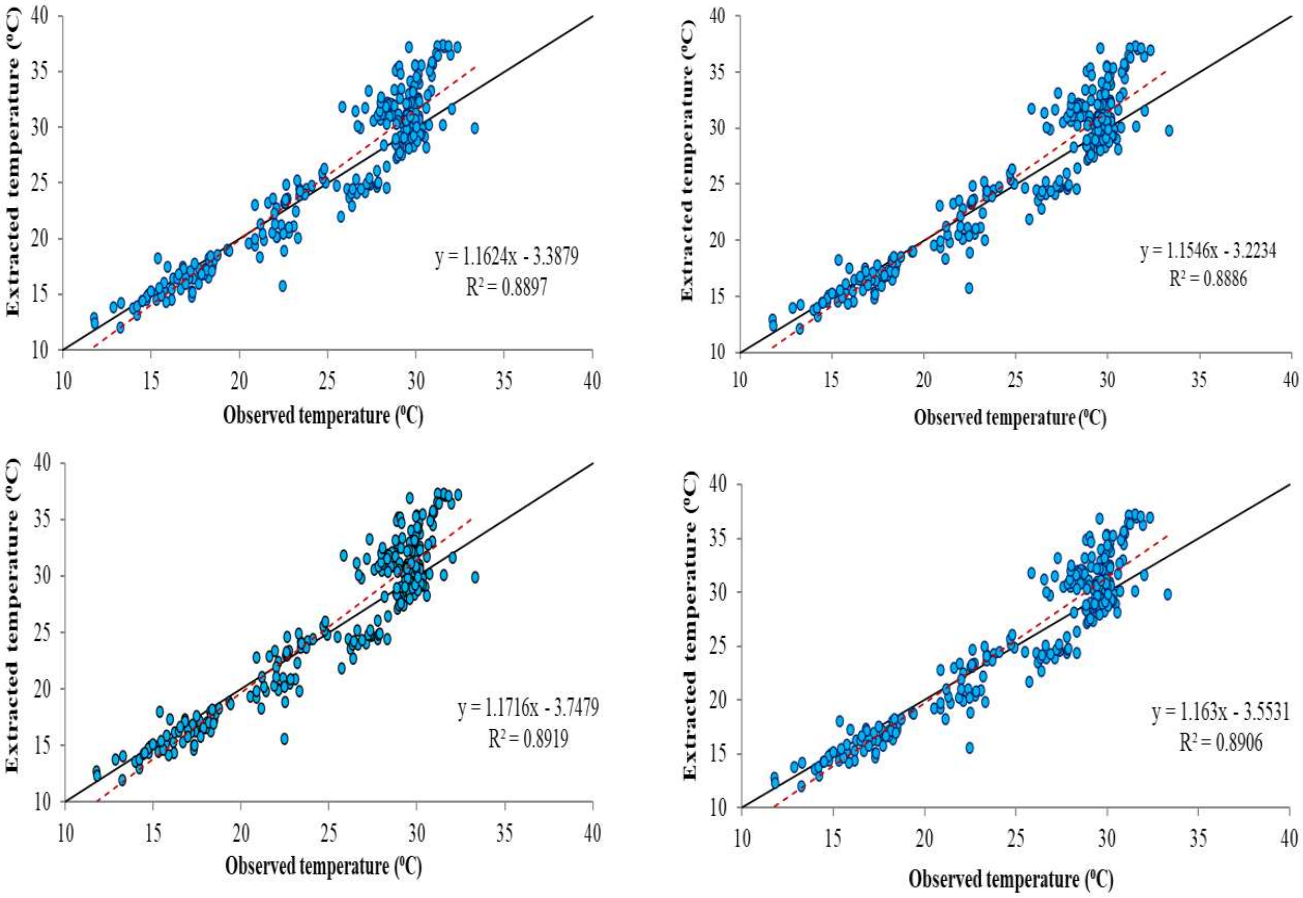

Fig. 4. Scatter plot between the observed mean temperature and that extracted from LST image at grid points

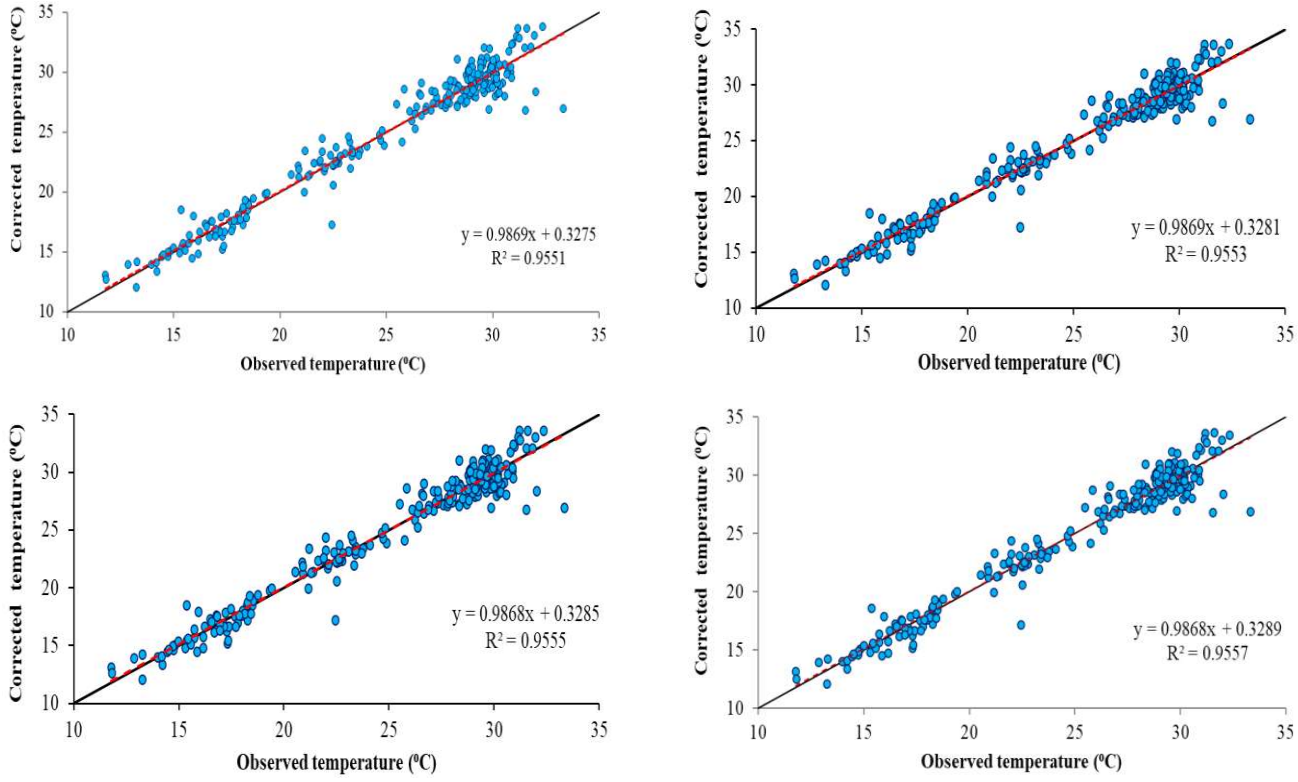

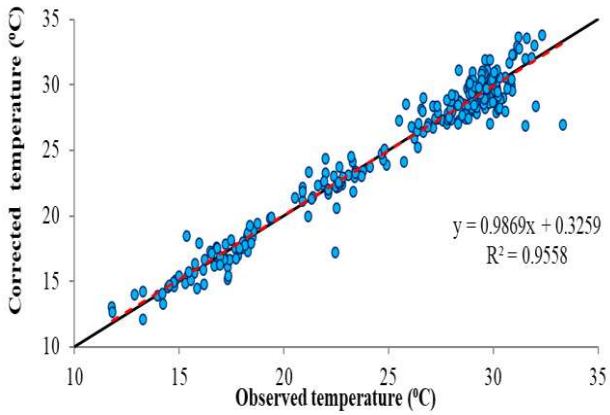
Corrected temperature (°C)
Observed temperature (°C)
y = 0.9869x + 0.3259
R² = 0.9558

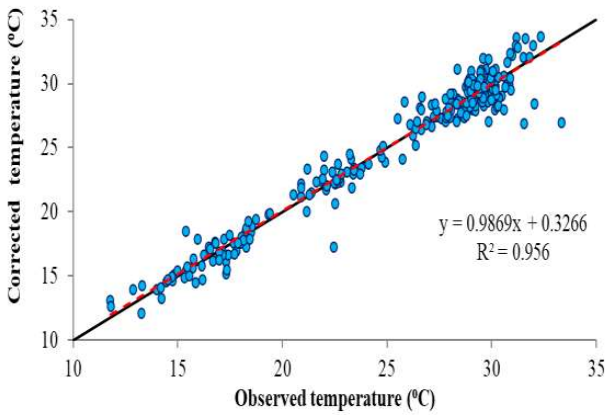
Corrected temperature (°C)
Observed temperature (°C)
y = 0.9869x + 0.3266
R² = 0.956

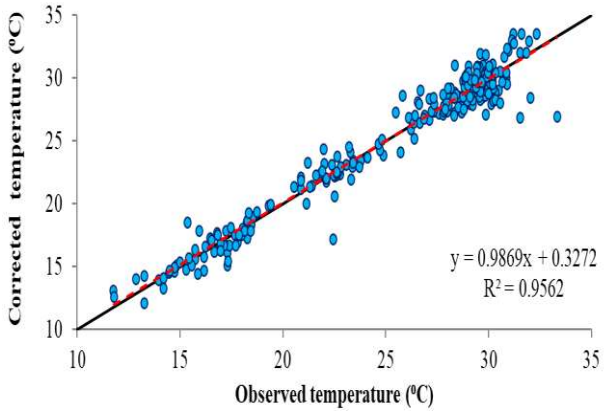
Corrected temperature (°C)
Observed temperature (°C)
y = 0.9869x + 0.3272
R² = 0.9562

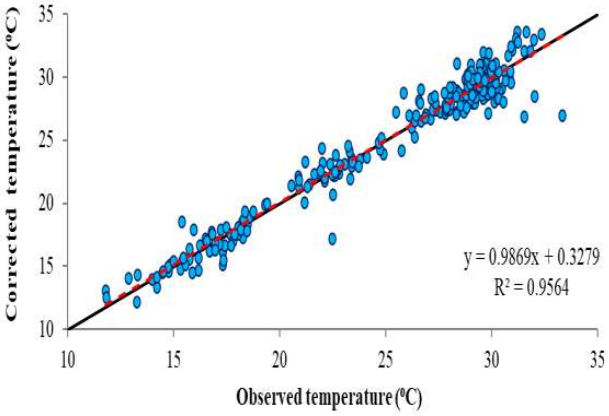
Corrected temperature (°C)
Observed temperature (°C)
y = 0.9869x + 0.3279
R² = 0.9564

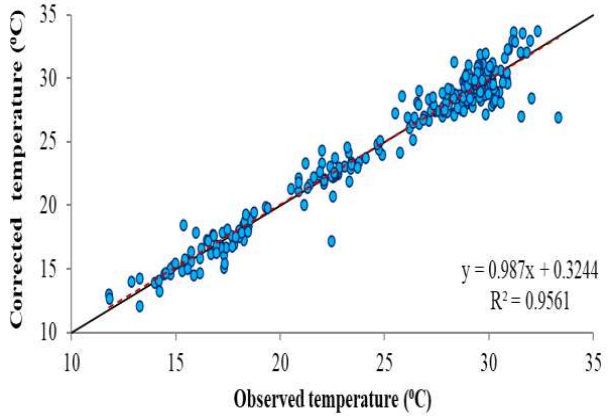
Corrected temperature (°C)
Observed temperature (°C)
y = 0.987x + 0.3244
R² = 0.9561

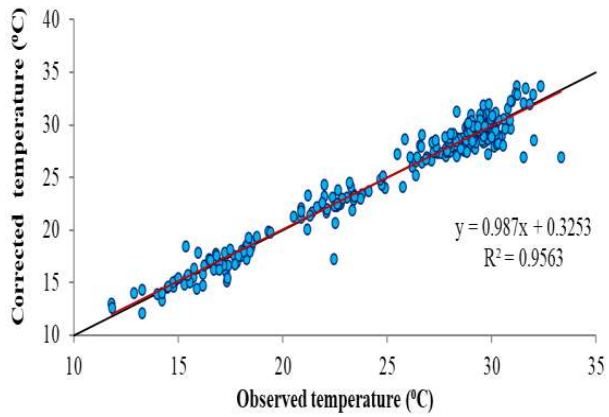
Corrected temperature (°C)
Observed temperature (°C)
y = 0.987x + 0.3253
R² = 0.9563

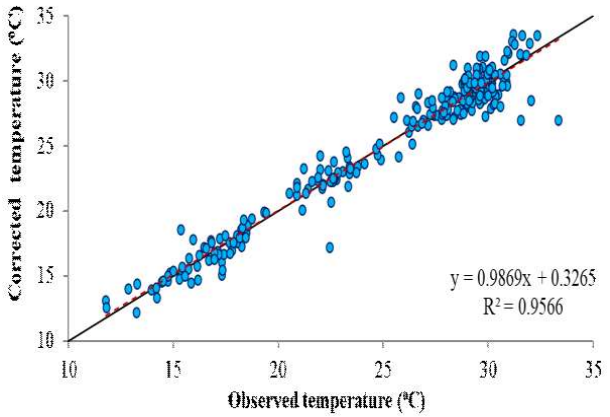
Corrected temperature (°C)
Observed temperature (°C)
y = 0.9869x + 0.3265
R² = 0.9566

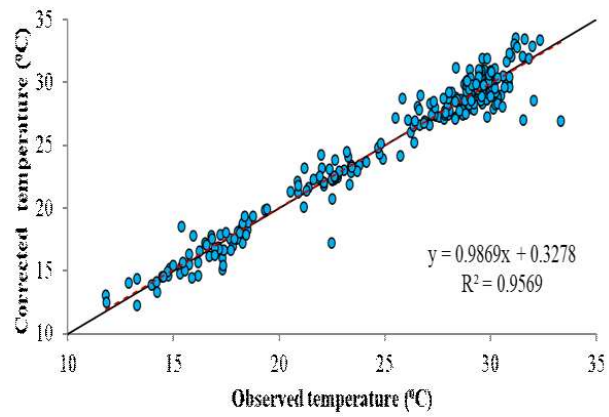
Corrected temperature (°C)
Observed temperature (°C)
y = 0.9869x + 0.3278
R² = 0.9569

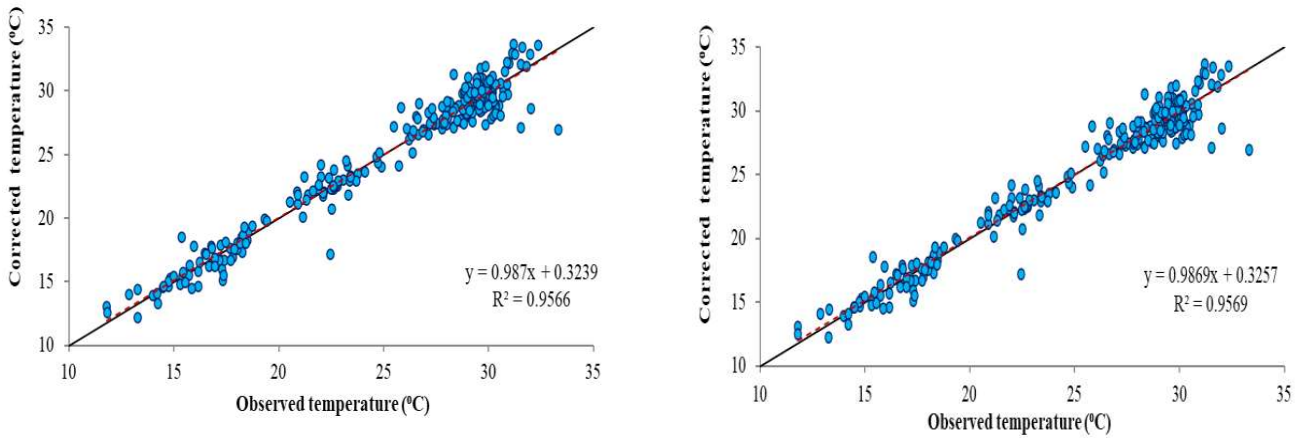

Fig. 5. Scatter plot between the observed and bias corrected mean temperature extracted from LST image at grid points

Table 3. Twenty years monthly average LST over study area

Month	LST (°C)	Month	LST (°C)	Month	LST (°C)
January	14.39	May	29.94	September	29.25
February	18.38	June	30.75	October	27.1
March	23.56	July	29.62	November	22.2
April	28.66	August	29.76	December	16.9

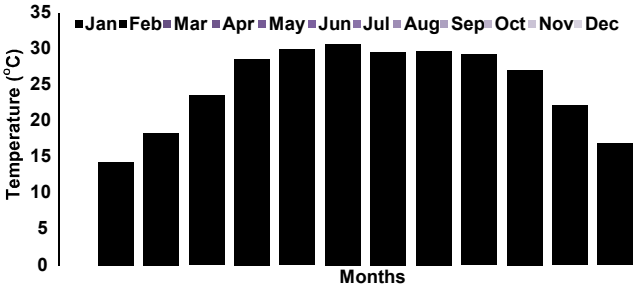

Fig. 6. Variation of temperature in the study area

land surface temperature over the study area was obtained by multiplying the AMFs to the land surface temperature extracted from GLDAS LST for each grid points and used to determine water surplus and deficit in the study area.

LST variation over study area presented in. The LST were maximum in the month of June (30.75°C) and minimum in January (14.39 °C) (Fig. 6 and Table 1). From January to July gradually increased and followed by decreasing trend from July to December (Fig. 7).

CONCLUSION

The monthly mean temperature estimated from the monthly dataset of Noah land surface temperature of Global Land Data Acquisition System (GLDAS) products of 0.25° × 0.25° grid size for the period of 2000 to 2020 using Arc Tool. The monthly air temperature for the months of January to December can be obtained by linear scaling of GLDAS LST product by multiplying the specific multiplying factors for each month. The statistical analysis advocates the use of satellites based GLDAS LST product for air temperature over the district however, application of statistical correction method like Linear-Scaling method of bias correction was found to be extremely suitable and reliable. The estimated LST was highest in the month of June (30.75 °C) and lowest in the month of January (14.39 °C) and from January to July, gradually increased and followed by decreasing trend from July to December. Future research must delve into seasonal temperature shifts, understanding causes and implications like the rise from January to July, followed by a decline to December. This analysis aids agricultural planning, water management, and climate adaptation. Extending studies beyond 2020 reveals long-term trends using high resolution temperature products is vital for assessing climate change impacts on local ecosystems, agriculture, and infrastructure.

REFERENCES

Ahmed K, Shahid S, Harun S and Nawaz M 2015. Performance assessment of different bias correction methods in statistical downscaling of precipitation. *Malaysian Journal of Civil Engineering* **27**(2): 311-324.

Bayissa Y, Tadesse T, Demisse G and Shiferaw A 2017. Evaluation of satellite-based rainfall estimates and application to monitor meteorological drought for the Upper Blue Nile Basin, Ethiopia. *Remote Sensing* **9**(3): 56-65.

Chung J, Lee Y, Jang W, Lee S and Kim S 2020. Correlation analysis between air temperature and MODIS land surface temperature and prediction of air temperature using tensor flow long short-

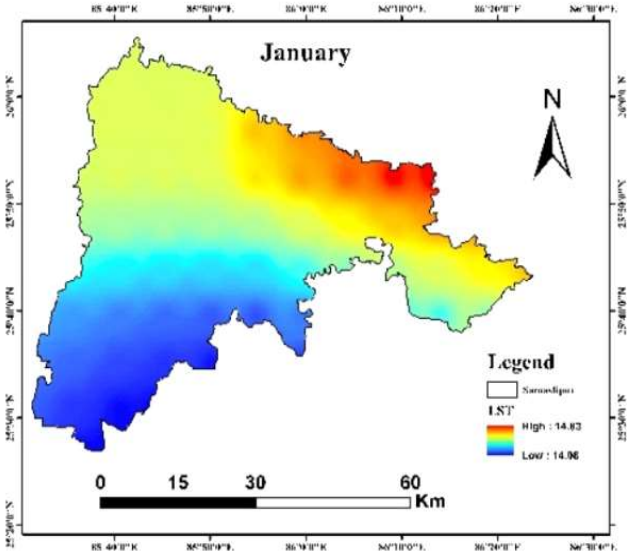
January
N
Legend
Samastipur
LST
High : 14.83
Low : 14.06
0 15 30 60
Km

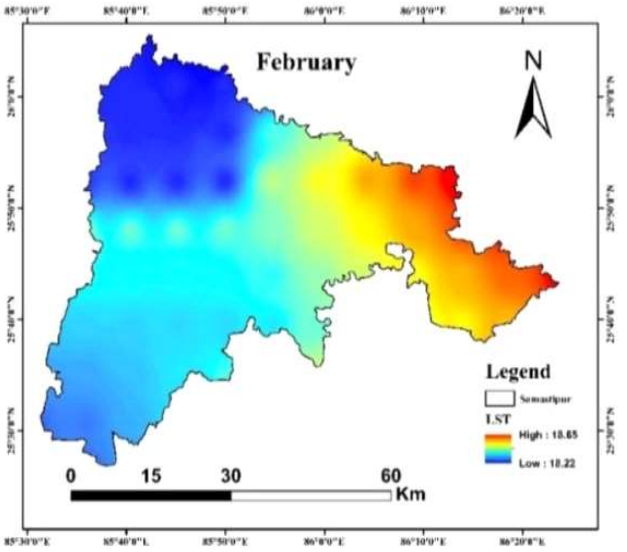
February
N
Legend
Samastipur
LST
High : 18.85
Low : 18.22
0 15 30 60
Km

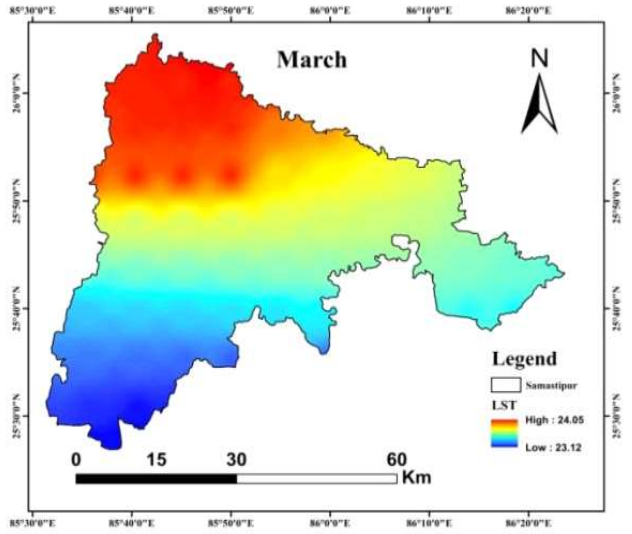
March
N
Legend
Samastipur
LST
High : 24.05
Low : 23.12
0 15 30 60
Km

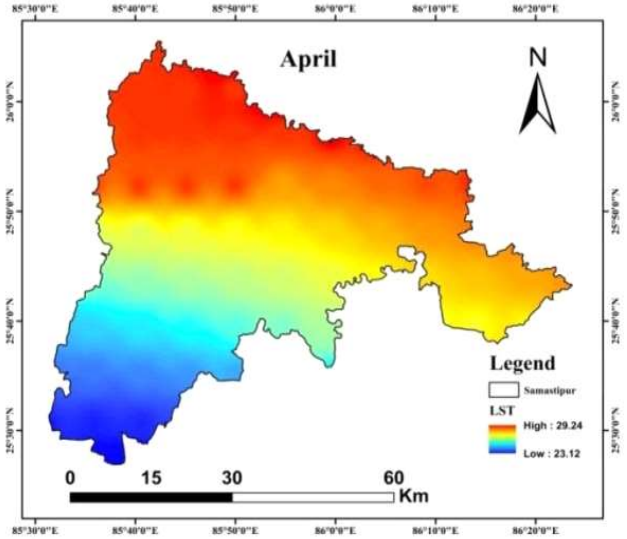
April
N
Legend
Samastipur
LST
High : 29.24
Low : 23.12
0 15 30 60
Km

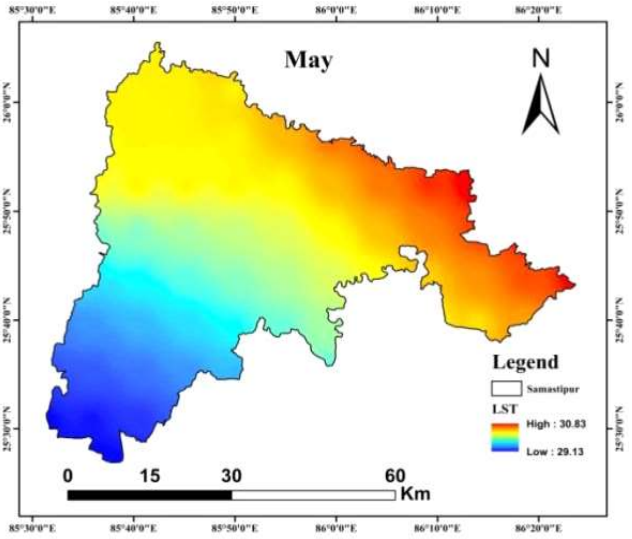
May
N
Legend
Samastipur
LST
High : 30.83
Low : 29.13
0 15 30 60
Km

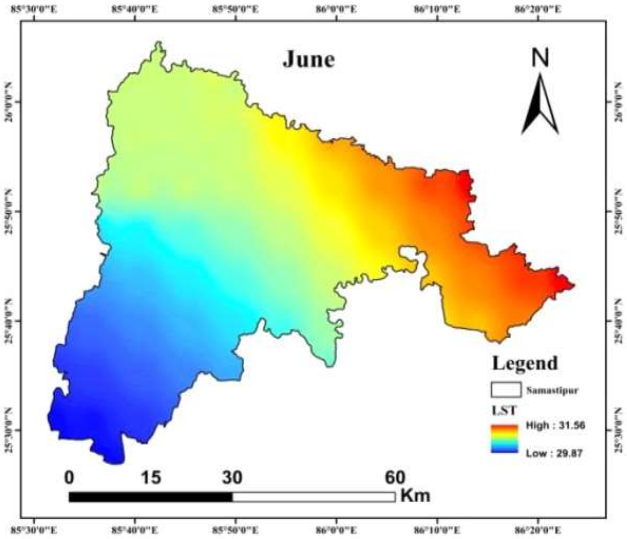
June
N
Legend
Samastipur
LST
High : 31.56
Low : 29.87
0 15 30 60
Km

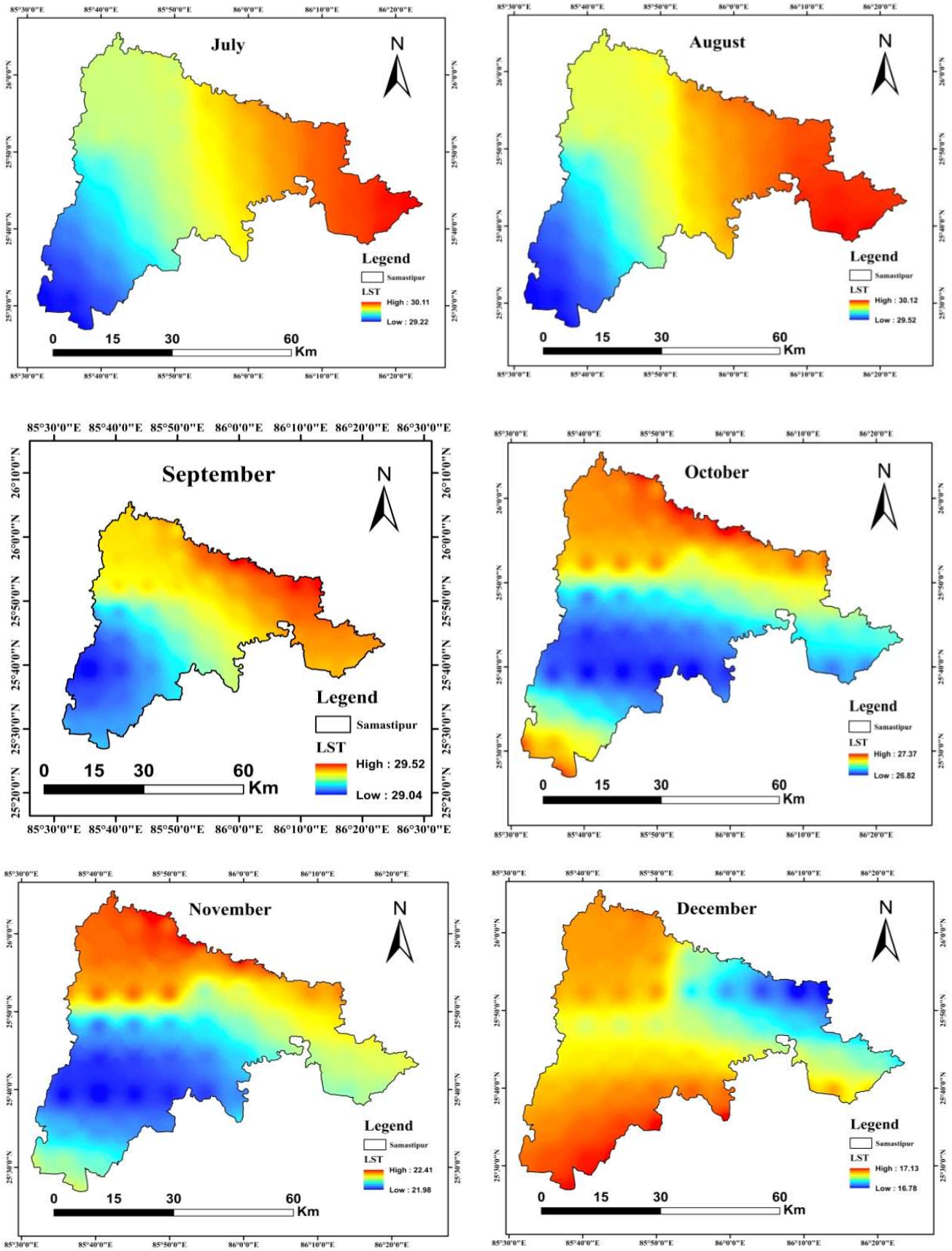

Fig. 7. Spatial distribution of 20 years average LST over the study area

term memory for the period of occurrence of cold and heat waves. *Remote Sensing* **12**(17): 3231-3245.

Deo RC and Şahin M 2017. Forecasting long-term global solar radiation with an ANN Algorithm coupled with Satellite-Derived (MODIS) Land Surface Temperature (LST) for regional locations in Queensland. *Renewable and Sustainable Energy Reviews* **72**(7): 828-848.

Li ZL, Tang BH, Wu H, Ren H, Yan G, Wan Z and Sobrino JA 2013. Satellite-derived land surface temperature: Current status and perspectives. *Remote Sensing of Environment* **131**(5): 14-37.

Li D and Wang L 2019. Sensitivity of surface temperature to land use and land cover change-induced biophysical changes: The scale issue. *Geophysical Research Letters* **46**(16): 9678-9689.

Meyer H, Katurji M, Appelhans T, Müller MU, Nauss T, Roudier P and Zawar-Reza P 2016. Mapping daily air temperature for Antarctica Based on MODIS LST. *Remote Sensing* **8**(9): 732-740.

Parinussa RM, Lakshmi V, Johnson F and Sharma A 2016. Comparing and combining remotely sensed land surface temperature products for improved hydrological applications. *Remote Sensing* **8**(2): 162-171.

Phan TN and Kappas M 2018. Application of MODIS land surface temperature data: A systematic literature review and analysis. *Journal of Applied Remote Sensing* **12**(4): 041501-041501.

Prasad S and Kumar V 2013. Evaluation of Fao-56 Penman–Monteith and alternative methods for estimating reference evapotranspiration using limited climatic data at Pusa. *Journal of Agrometeorology* **15**(1): 22-29.

Prasad S, Kumar V, AK Sinha and Singh AKP 2012. Evaluation of hargreaves method for estimating reference evapotranspiration at Pusa, India. *International Agricultural Engineering Journal* **21**(4): 90-95.

Singh A, Sahoo RK, Nair A, Mohanty UC and Rai RK 2017. Assessing the performance of bias correction approaches for correcting monthly precipitation over India through coupled models. *Meteorological Applications* **24**(23): 326-337.

Subramanya 2006. *Engineering Hydrology, 2nd Edition*, Tata McGraw Hill, Publishing Company Ltd., New Delhi, India, p 127.

Wan Z 2006. MODIS Land Surface Temperature Products Users Guide. *Institute for Computational Earth System Science,* University of California: Santa Barbara, CA, USA, p805.

Yang JS, Wang YQ and August PV 2004. Estimation of land surface temperature using spatial interpolation and satellite-derived surface emissivity. *Journal of Environmental Informatics* **4**(1): 37-44.

Zeng L, Wardlow BD, Tadesse T, Shan J, Hayes MJ, Li D and Xiang D 2015. Estimation of daily air temperature based on MODIS land surface temperature products over the corn belt in the US. *Remote Sensing* **7**(12): 951-970.

Received 16 September, 2023; Accepted 28 December, 2023